Estimating actual evapotranspiration from stony-soils in montane ecosystems

Kshitij Parajuli[1,2*], Scott B. Jones[2], David G. Tarboton[1], Gerald N. Flerchinger[3], Lawrence E. Hipps[2], L. Niel Allen[1], Mark S. Seyfried[3]

[1] Dept. of Civil and Environmental Engineering, Utah State University, Logan, UT

[2] Dept. of Plant Soils and Climate, Utah State University, Logan, UT

[3]Northwest Watershed Research Center, USDA-ARS, Boise, ID

[*]Email: parajuli@usu.edu, kshparajuli@gmail.com

Highlights

i) Numerical simulation of actual evapotranspiration (ET) from natural/montane ecosystems

ii) Stone hydraulic properties reveal contribution to soil water availability

iii) Effect of soil stone content on actual evapotranspiration was quantified

Abstract

Quantification of evapotranspiration (ET) is crucial for understanding the water balance and for efficient water resources planning. Agricultural settings have received much attention regarding ET measurements while there is less knowledge regarding actual ET (ET_A) in natural ecosystems. This study is focused on modelling ET_A from stony soil, particularly in montane ecosystems where we estimate the contribution of stone content on water retention properties in soil. We employed a numerical model (HYDRUS-1D) to simulate ET_A in natural settings in northern Utah and southern Idaho during the 2015 and 2016 growing seasons based on meteorological and soil moisture measurements at a range of depths. We simulated ET_A under three different scenarios, considering soil with (i) no stones, (ii) highly porous stones, and (iii) negligibly porous stones. The simulation results showed significant overestimation of modeled ET_A when neglecting stones in comparison to ET_A measured by eddy covariance. Modeled ET_A estimates with negligibly porous stones were much lower for all cases due to the substantial decrease in soil water storage compared with estimates made considering highly porous stones. Assumptions of highly porous or negligibly porous stones lead to reductions in simulated ET_A of between 10% and 30%, respectively, compared with no stones. These results reveal the important role played by soil stones, which can impact the water balance by altering available soil moisture and thus ET_A in montane ecosystems.

***Keywords*:** Evapotranspiration, Forest soil, HYDRUS-1D, Stony-soil, Montane ecosystems

1. Introduction

Evapotranspiration (ET) is the largest outward flux of water and a key component of the hydrological cycle and is therefore essential in quantifying the water budget and planning water resources (Baldocchi and Ryu, 2011; Mu et al., 2007; Schelde et al., 2011; Sheffield et al., 2010). Water flux to the atmosphere by the process of ET constitutes up to 95% of the water balance in arid regions (Kool et al., 2014; Wilcox et al., 2003). However, ET remains a major source of uncertainty in eco-hydrological systems, and this uncertainty motivates research on more accurate quantification of ET within large-scale irrigated projects and natural ecosystems. Forests have been recognized as a fundamental part of ecosystems that play a key part in regulating hydrological balance by altering streamflow and ET (Andreassia 2004; Ice and Stednick, 2004; Parajuli et al., 2019; Sun et al., 2008). Despite the fact that many studies have been conducted on ET estimation across different spatial scales ranging from point- to basin-scale (Parajuli 2015; Senay et al., 2011; Schelde et al., 2011), very few focused on natural ecosystems as compared to agricultural settings. Accurate quantification of ET in natural ecosystems is essential to evaluate the effects of land management and global change on availability of water, streamflow, and ecosystem productivity (Andreassia 2004; Parajuli 2018; Sun et al., 2008; Zhou et al., 2008).

Correct information about temporal and spatial variations in ET is critical for better understanding of the interactions between land surfaces and the atmosphere and solving the water and energy balances used in hydrological and climate models (Kumar et al., 2006; Mu et al., 2007; Niu et al., 2011; Yang et al., 2011). Better estimates of ET are furthermore important to improve management of water resources and agricultural systems by assisting in decision making processes related to water allocations (Allen et al., 1998; Kumar et al.,

2006; Mu et al., 2007, Raziei and Pereira, 2013). However, it is challenging to calculate ET over land surfaces characterized by heterogeneity in soil and vegetation type and in other parameters affecting the ET (Mu et al., 2007; Senay et al., 2011; Sheffield et al., 2010; Sun et al., 2008).

A number of techniques to estimate ET have been developed, such as the catchment water budget method using soil and plant weighing lysimeters as well as the Bowen ratio and eddy covariance methods, which have been developed and applied at different scales (Prueger et al., 1997; Wilson et al., 2001). Watershed ET measurements using a catchment scale water budget approach, where ET is calculated as the residual of the water balance (Baldocchi and Ryu, 2011), depend on the reliability and accuracy of other observations such as precipitation, runoff, drainage and infiltration. Lysimeters on the other hand can provide actual ET (ET_A) by measuring weight change, though their installation and maintenance costs are high. The surface energy balance approach and eddy covariance technique provide alternatives to measure ET_A at spatial- and point-scales, while their applications are limited due to the requirement of intensive measurements and information about energy balance components (Law et al., 2002; Wilson et al., 2001). The latent heat flux data collected at eddy covariance towers are considered as validation of the results from hydrologic models at point- as well as regional-scales (Baldocchi et al., 1988; Wilson et al., 2001).

Various analytical models have been developed to estimate ET where there are no direct measurements. A widely used model is the Penman-Monteith (PM) equation that calculates ET for a leaf or complete cover canopy based on observed meteorological parameters such as net radiation, wind speed and saturation deficit. The equation also includes turbulence

characteristics by considering aerodynamic resistance and plant physiology via stomatal resistance, both of which are difficult to determine. The PM equation can be used to estimate reference ET (ET_o), which represents the hypothetical ET of a short green crop (grass) that fully covers the ground with unlimited water availability, and has arbitrarily low stomatal resistance (Allen et al., 1998). The ET_o is estimated based on meteorological parameters and does not depend on soil water and vegetation. The actual ET (ET_A) will differ and is usually less, due to limited soil moisture or stomatal response to the natural ecosystem environment. As available soil moisture affects many ecological and environmental processes including ET, in principle, ET can be quantified by studying the soil moisture dynamics (Cai et al., 2017; Koster et al., 2004; Lv et al., 2014; Miyazawa et al., 2013; Wilson et al., 2001).

There are numerical modeling approaches that can estimate ET_A by accounting for soil moisture dynamics in the simulation of plant root water uptake and surface evaporation. HYDRUS-1D is one such model that has been widely used for simulating ET_A (Hilten et al., 2008; Hlaváčiková and Novák 2013; Ries et al 2015; Sadeghi et al., 2019; Solyu et al., 2011; Sutanto et al., 2012). HYDRUS-1D is a physically based finite-element model for simulating one dimensional flow of heat and water in variably saturated media that numerically solves the modified Richards equation (Richards, 1931) accounting for root water uptake as a sink term (Simunek et al., 2016). The model is able to simulate water flow in and out of the soil when adequate soil and vegetation parameters are provided. Both soil and vegetation are however, extremely diverse in montane ecosystems. Soil hydraulic properties vary horizontally and vertically due to non-uniformity in soil properties, representation of which requires detailed information on soil parameters to simulate the

106 soil water flow and root water uptake (Mohanty 2013). An advantage of the HYDRUS-1D
107 model is that it can inversely fit the soil hydraulic parameters when the measured soil water
108 content, matric potential or other relevant information is provided (Simunek et al., 2016).

109 Apart from the variation in soil texture, non-arable soils contain significant quantities of
110 stone fragments (particles with diameter >2 mm) that may modify the water storage
111 capacity of soil. Stones furthermore alter the soil hydraulic transport properties, which in
112 turn affect the available water for root uptake (Cousin et al., 2003; Novak and Knava,
113 2012). Higher stone content is expected to reduce the soil water storage capacity of stony
114 soils in comparison to the fine soil matrix (soil constituents below 2 mm in diameter;
115 Hlaváčiková et al. 2016; Novak et al., 2011; Parajuli et al., 2017a) when the stone porosity
116 is lower. Stones reduce the available water for root uptake and hence limit the rate of ET
117 (Novak and Knava, 2012; Parajuli et al., 2017; Tetegan et al. 2011). Many studies in the
118 past have neglected the presence of soil stone fragments when simulating soil moisture
119 dynamics. Two different approaches are common while dealing with stony soils. One
120 assumes the stones as a non-porous system, hence any water held by the stones is not
121 accounted for. This leads to reduced water estimation per unit volume as pointed out by
122 Cousin et al. (2003) and Ugolini et al. (1998). Plant available soil water in such cases may
123 be underestimated by up to 34% according to Cousin et al. (2003). By contrast, the second
124 approach essentially considers the stones as behaving similar to the fine soil matrix, which
125 typically has a higher water holding capacity than stones. In Cousin et al. (2003), plant
126 available water was overestimated by 39% using this second approach. It may therefore be
127 important to consider the contribution of stone fragments to soil water storage when

simulating soil moisture dynamics involving ET estimation, especially when soil stone content is significant.

The objectives of this research involved: (1) Modelling ET_A using the physically based numerical model, HYDRUS-1D, and validating its output against eddy covariance measurements. (2) Examining the effect of stone content on estimation of ET_A from natural vegetation in stony soils. (3) Comparing simulated ET_A for cases; i) neglecting the presence of stones, ii) considering highly porous soil stone content and iii) considering negligibly porous stone content.

2. Site Description

In this study, we selected four climate stations in northern Utah and one in southern Idaho as shown in Figure 1. The location and general vegetation around the stations are presented in Table 1. The stations in Utah are part of the innovative Urban Transitions and Arid region Hydro-sustainability (iUTAH) project. The iUTAH project has developed and installed several weather- and aquatic-stations to monitor and understand Utah's water resources. These are referred to as GAMUT sites as they are intended to quantify processes on a Gradient Along Mountain to Urban Transition (GAMUT). These stations measure different aspects of climate, hydrology, and water quality in three watersheds (Logan River-, Red Butte Creek- and Provo River-Watersheds; iUTAH 2014; Jones et al., 2018).

The climate of northern Utah and southern Idaho is typical of the montane semi-arid intermountain west and varies widely with four distinct seasons: cold snowy winter, hot dry summer and transition periods of spring and autumn. The majority of precipitation occurs as snowfall. The higher elevation weather stations are covered with snow until May

150 or June whereas early snowmelt occurs at weather stations in lower elevations. Patches of
151 sagebrush surround the observation sites at Tony Grove, Beaver Divide and Soapstone,
152 while the Knowlton Fork station is located in a sloping meadow surrounded by tall ferns.
153 The meteorological parameters required for calculating ET_o (reference ET), such as air
154 temperature, saturation deficit, net radiation and wind speed were recorded every fifteen
155 minutes. In addition, the soil moisture and temperature were measured at depths of 5-, 10-,
156 20-, 50-, and 100- cm using time-domain-transmissometry (TDT) at the same time step as
157 the meteorological parameters (iUTAH 2014). Blonquist et al., (2005) and Jones et al.,
158 (2005) provide detailed description of the measurement principles of TDT, where the
159 permittivity - soil moisture calibration is based on the Topp et al. (1980) equation.

160 The Low Sage site is part of the Critical Zone Observatory (CZO) located in Reynolds
161 Creek Experimental Watershed of southwestern Idaho, approximately 80 km southwest of
162 Boise, Idaho, USA. The site was equipped with sensors to collect meteorological and soil
163 data along with an eddy covariance tower to quantify water and carbon fluxes in a
164 sagebrush ecosystem. Short and long wave radiation, air temperature and humidity were
165 collected at the eddy covariance station every 30 minutes using a four-component net
166 radiometer (CNR-1, Kipp and Zonen, Delft, The Netherlands), and a temperature/humidity
167 probe (HMP155C, Vaisala, Helsinki, Finland). Ground heat flux was measured with six
168 heat flux sensors (HFT3, REBS, Seattle, WA) installed 0.08-m deep within the soil and
169 three sets of self-averaging thermocouples installed at 0.02 and 0.06-m deep (Fellows et
170 al., 2017). The meteorological station near the EC tower includes measurements of air
171 temperature, humidity, wind speed and direction and solar radiation. Weather and soil data
172 were processed at 30-minute intervals. Precipitation was measured and aggregated hourly

using a dual-gauge system especially designed for windy and snow dominated conditions. Volumetric soil water content was recorded every hour at mean depths of 5-, 15-, 30-, 60-, and 90-cm.

During installation of soil moisture sensors at each station, the excavated soil was analyzed in order to determine the soil texture, root distribution and stone content (Parajuli et al., 2017b; Patton et al., 2018). The soil description for the selected stations exhibited a high degree of heterogeneity along the depth with significant volumetric stone content (v). Information on vertical distribution of stone content and root density derived from the soil pit description at each site is presented in Figure 2.

Soil pit descriptions extended from the surface to 100 cm deep in most of the stations. Stone content in the bottommost layer was assumed to extend down to 200 cm, the bottom boundary for numerical simulations. As shown in Figure 2, Low Sage, Tony Grove, Knowlton Fork and Soapstone exhibited around 0.45 $m^3\ m^{-3}$ volumetric stone content between the depth of 40- to 80-cm. Average stone content within a one-meter soil profile ranged from 0.07 $m^3\ m^{-3}$ at Knowlton Fork to 0.38 $m^3\ m^{-3}$ at Tony Grove. The majority of stones collected from soil pits in the iUTAH stations were sandstone with variation in their individual porosities. Sandstones with coarser grains had higher porosities, close to thirty percent and exhibited water retention properties similar to sandy soil. However, fine grained sandstones were negligibly porous with porosities between three to five percent. The water retention properties of the stones were measured by Parajuli et al. (2017a) and are presented in Table 2.

3. Theoretical Considerations

3.1 HYDRUS-1D Numerical Modeling

In this study we used HYDRUS-1D software (Version 4.17, Simunek et al., 2013), which simulates variably-saturated water flow in soil using the modified Richards equation expressed as:

$$\frac{\partial \theta(h)}{\partial t} = \frac{\partial}{\partial z}\left[K(h)\left\{\frac{\partial h}{\partial z} + 1\right\}\right] - S \qquad (1)$$

where θ is volumetric water content [$L^3\ L^{-3}$], z is the vertical coordinate [L], t is time [T], h is the soil matric potential [L], $K(h)$ is the unsaturated hydraulic conductivity function [$L\ T^{-1}$] and S is a sink term [$L^3\ L^{-3}\ T^{-1}$].

The variable boundary condition in HYDRUS-1D was governed by the effective precipitation, and actual flux exchange at the soil-atmosphere interface was driven by the atmospheric demand and controlled by the near-surface soil moisture described further in Simunek et al. (2013). The reference evapotranspiration (ET_o) was calculated using the FAO-recommended Penman-Monteith combination equation using meteorological parameters (Allen et al., 1998; FAO, 1990; Monteith and Unsworth, 1990) and partitioned into potential evaporation (E_p) and potential transpiration (T_p) fluxes using Beer's Law (Ritchie 1972):

$$T_p = ET_o \cdot \left(1 - e^{-k \cdot LAI}\right) = ET_o \cdot SCF \qquad (2)$$

$$E_p = ET_o \cdot (e^{-k \cdot LAI}) = ET_o \cdot \left(1 - SCF\right) \qquad (3)$$

where the soil cover fraction, $SCF=1-exp(-k\ LAI)$, k is the radiation extinction coefficient (set to 0.463 for this study) and LAI is leaf area index (Simunek et al., 2013).

The sink term, S in Equation (1) represents the volume of water lost from the soil in unit time due to root water uptake (Feddes et al., 1978) and calculated as (Simunek et al., 2013):

$$S(h,z) = \alpha(h,z)b(z)\cdot S_p \quad (4)$$

where $\alpha(h,z)$ is the root-water uptake stress response function (Feddes et al., 1974, 1978). S_p is the potential water uptake rate [T^{-1}]. The normalized root-water uptake distribution function, $b(z)$, describes the relationship between root-water uptake and root density distribution. The root distribution based on root counts from the soil pit description exhibits substantial variability from site to site and is unlikely to redevelop similarly given the disturbed soil being returned to the pit, thus root distribution from pit descriptions are not an ideal representation (Figure 2). Hence we used the Hoffman and van Genuchten (1983) method estimates as described in Simunek et al. (2013) in this study. Most of the selected sites were mixed grass and sagebrush at all weather stations as indicated in Table 1. The maximum crop height was considered to be 1 m with albedo 0.17 and surface roughness values of 0.001 m as suggested by Simunek et al. (2013).

The lower boundary condition was set as a free drainage boundary, assuming an infinitely deep soil profile with no effect of ground water table. The initial conditions were described by the measured initial moisture content along the soil profile at time $t = 0$. The surface boundary condition of the soil domain was set to the atmospheric boundary condition with surface runoff. The soil parameters for the van Genuchten-Maulem water retention model (Mualem 1976; van Genuchten 1980) were calibrated for each layer using inverse modelling in HYDRUS-1D. The van Genuchten (1980) model is expressed as;

$$S_e = \frac{\theta - \theta_r}{\theta_s - \theta_r} = \left[1 + \left(\alpha|h|\right)^n\right]^{-m} \quad (5)$$

where S_e is the effective degree of saturation [-], θ_r and θ_s are the residual and saturated volumetric water contents [$m^3\ m^{-3}$], α is a factor related to the inverse of the air entry pressure [m^{-1}], and n and m are empirical fitting parameters related to the soil pore-size distribution.

The HYDRUS-1D numerical model was initialized using the soil hydraulic parameters obtained from field estimates. The soil profile was divided into five layers with one soil moisture sensor in each layer. The first step was to calibrate the model without the effect of stone content assuming the total soil profile was comprised of fine soil alone. The initial soil hydraulic parameters (θ_r, θ_s, α, n and K_s) were estimated using Rosetta Lite v1.1 software in HYDRUS-1D, based on the sand, silt and clay fractions of fine soil obtained from soil pit descriptions (Parajuli et al., 2017b; Patton et al., 2018). If the Rosetta Lite predictions of θ_r and θ_s values were above the lowest or below the highest measured soil moisture values in each layer, the minimum or maximum measured values were set as θ_r or θ_s, respectively. Model calibration was achieved primarily by inversely fitting the soil hydraulic parameters (α, n and K_s) for each of the 5 soil layers.

3.2. Accounting for Stone Content in the HYDRUS-1D Simulation

In order to address the impact of stone content on soil hydraulic properties and thus estimation of ET_A, the stony soil was assumed to be a binary porous medium allowing two different water retention properties for stone and fine soil in each layer. The dual porosity water retention model (Durner 1994), which assumes equilibrium conditions, was applied to satisfy the algorithm suggested by Parajuli et al., (2017a) to account for the effect of stone fragments in the soil.

$$\frac{\theta_{mix}-\theta_{r_{mix}}}{\theta_{s_{mix}}-\theta_{r_{mix}}} = w_{so}\left[1+\left(\alpha_{so}h\right)^{n_{so}}\right]^{-m_{so}} + w_{st}\left[1+\left(\alpha_{st}h\right)^{n_{st}}\right]^{-m_{st}} \quad (6)$$

where the parameters with subscript *so*, *st* and *mix* are van Genuchten parameters for fine soil fraction, stone inclusion and soil-stone mixture, respectively. The weighting factors for soil and stone fractions, w_{so} and w_{st}, at saturation are defined as:

$$w_{so} = \frac{(1-v)\theta_{s,so}}{(1-v)\theta_{s,so}+v\theta_{s,st}} \quad (7)$$

$$w_{st} = \frac{v\theta_{s,st}}{(1-v)\theta_{s,so}+v\theta_{s,st}} \quad (8)$$

where v is the ratio of the stone fragment volume to the total soil volume (or volume fraction of stone content).

In order to understand the impact of variably porous stones in simulation of ET_A, two scenarios were studied where all the stones were considered as either coarse sandstones (highly porous) or fine sandstones (negligibly porous) with water retention properties expressed in Table 2.

The unsaturated hydraulic conductivity as a function of the stony soil effective saturation is defined by combining Eq. (6) with Mualem's (1976) pore-size distribution model as suggested by Durner et al. (1999):

$$K(S_{e,mix}) = K_s \frac{(w_{so}S_{e_{so}}+w_{st}S_{e_{st}})^{l}(w_{so}\alpha_{so}[1-(1-S_{e_{so}}^{1/m_{so}})^{m_{so}}]+w_{st}\alpha_{st}[1-(1-S_{e_{st}}^{1/m_{st}})^{m_{st}}])^{st}}{(w_{so}\alpha_{so}+w_{st}\alpha_{st})^{2}} \quad (9)$$

where l is empirical parameter of the hydraulic function.

4. Results

4.1 Calibration of the HYDRUS-1D model

The soil hydraulic parameters were optimized for different soil layers as described in Section 3.1 without considering the effect of stone content at each monitoring station. The initial as well as optimized soil hydraulic parameters at different depths are provided as supplementary material. The simulation period started following snowmelt, when the soil moisture was near field capacity. The Low Sage station in Idaho had early snowmelt allowing us to initialize the model on DOY 100 (10 April 2015), while iUTAH stations in Northern Utah were snow covered until about the middle to the latter part of May. In order to compare the same time period, simulations started on DOY 148 (28 May 2015) at all iUTAH stations running until the end of September (DOY 274). The same period was selected for both years to have better comparison of ET estimates under different conditions. Daily precipitation plotted in Figure 3 shows that 2016 experienced much less rainfall than 2015. The four iUTAH stations illustrated in Fig. (1) have recorded similar rainfall patterns over the period. There were several rain events during the simulation period in 2015, but 2016 remained relatively dry with one major precipitation event towards the end of September (DOY 268).

Measured volumetric water content and HYDRUS-1D simulations of water content at soil profile depths of 5-, 15-, 30-, 60-, and 90-cm from the Low Sage station are presented in Figure 4. Variation in rainfall is expected to alter the soil moisture dynamics in both years. The volumetric water content approached the saturation level during spring snowmelt, but these montane soils drain quickly to field capacity once snowmelt ceases. Rain events during the summer of 2015 recharged the soil profile to a depth of 30 cm as shown in

299 Figure 4. There was no significant rain event during the simulation period in 2016, and the
300 soil dried down towards the end of the growing season.
301 Simulation results for the four iUTAH sites using HYDRUS-1D are compared with TDT
302 measured soil moisture contents at 5-, 10-, 20-, 50-, and 100-cm in Figure 5. Soil moisture
303 dropped rapidly from a near-saturated condition at the beginning of the growing
304 season/simulation period. Similar to Figure 4, the sensors at depths 5-, 10- and 20-cm
305 reflected the effect of rainfall with rapid rise in moisture content readings during 2015;
306 however, the amount of precipitation was not enough to wet the sensors below 20 cm
307 throughout the growing season.
308 The goodness of fit to the measured soil moisture values with the HYDRUS-1D simulation
309 are expressed in terms of coefficients of determination (R^2) and root mean squared errors
310 (RMSE) shown in Table 3. The calibrated HYDRUS-1D simulation results compared well
311 with measured soil moisture at each depth for both years. The coefficients of determination
312 (R^2) were greater than 0.8 for most depths, while a few of the simulation depths had R^2 as
313 low as 0.65 (Table 3). The RMSE remained less than 0.04 $m^3\ m^{-3}$ on average for all the
314 stations. The few R^2 values below 0.8 and RMSE values greater than 0.03 $m^3\ m^{-3}$ for
315 individual depths are bolded for clarity in Table 3. The match between simulated and
316 observed water contents at different depths in all stations suggests the HYDRUS-1D model
317 hydraulic parameters were well calibrated to represent the soil hydrodynamics.
318 **4.2 Simulation of Actual Evapotranspiration**
319 At first the root water uptake and evaporative fluxes from soil and plants were simulated
320 by HYDRUS-1D to provide an estimate of the ET_A without considering the effect of stones.
321 Daily ET_A estimates simulated by HYDRUS-1D were compared with eddy covariance

measurements of ET_A at the Low Sage station as illustrated in Figure 6. The daily ET_A simulated by the HYDRUS-1D model followed the seasonal patterns of eddy covariance measured ET_A very well (Figure 6). The correlation between the eddy covariance measurements and the HYDRUS-1D simulation of ET_A without stone content effects was found to have an R^2 of 0.78 and 0.76 for years 2015 and 2016, respectively (Figure 7, Table 4). Similarly, the RMSE values for 2015 and 2016 were 0.64 mm/day and 0.51 mm/day, respectively (Table 4). The HYDRUS-1D model periodically overestimated ET_A compared to the eddy covariance measurements, mostly around rain events. The cumulative ET_A measured by eddy covariance for the period DOY 101 (10 April) to DOY 273 (30 September) was 305 mm and 221 mm in 2015 and 2016, whereas the HYDRUS-1D simulation estimated 332 mm and 198 mm in 2015 and 2016, respectively. This overestimation of ET_A simulated by HYDRUS-1D in 2015 and the underestimation in 2016 is also evident from the scatter plot for the no stones condition shown in Figure 7. However, the seasonal total ET_A values from HYDRUS-1D were in good agreement with the eddy covariance results.

4.3. Effect of Stone Content on Evapotranspiration

With the aim of analyzing the impact of stone content on ET_A, we simulated three different scenarios assuming soil for all five sites with: no stones; highly porous stones (Coarse Sandstone); and negligibly porous stones (Fine Sandstone). The average stone content for each layer was estimated based on the soil pit description also presented in Figure 2. The water retention parameters for the highly and negligibly porous stone considered for this study were measured in the laboratory (Parajuli et al., 2017a) and are presented in Table 2.

345 The simulation in the Low Sage site where the average stone content was 0.18 $m^3 m^{-3}$
346 showed substantial improvement in estimation of ET_A, when the stones were considered
347 as negligibly porous stones. The R^2 values increased slightly while RMSE values were
348 lower under the negligibly porous stone scenario for both years (Table 4). The result
349 supported our assumption, namely, that if we could quantify the stone content in the soil
350 properly and include that in the soil moisture simulation, the ET_A from stony soil would be
351 estimated more accurately.
352 Figure 8 shows the cumulative ET_A simulated by HYDRUS-1D under the three different
353 scenarios considering soil with no stone, highly porous stone and negligibly porous stone
354 at each station. With the purpose of comparing ET_A over the same period for each site, the
355 cumulative ET is presented from DOY 148 (28 May) to DOY 273 (30 September) for all
356 stations. In general, the cumulative ET_A over the same period in 2016 is much less than
357 that from 2015 for all stations providing us with the impression that the available soil
358 moisture limited the ET_A. The year 2016 was considerably drier than 2015, resulting in
359 reduced soil water storage, which is also implicit in Figure 4 and 5.
360 The simulations under different conditions revealed significant reductions in cumulative
361 ET_A at the Tony Grove and Soapstone stations. The percent changes in simulated actual
362 transpiration (T_A), evaporation (E_A) and ET_A for conditions with highly porous stones and
363 negligibly porous stones with reference to soil without stones, is presented in Table 5. The
364 cumulative ET_A was reduced by 10% and 21% at Tony Grove and 1% and 17% at
365 Soapstone for assumptions of highly- and negligibly-porous stones, respectively (Table 5).
366 However, there was not any noticeable change in cumulative ET_A at the Knowlton Fork
367 station where the average stone content was 0.07 $m^3 m^{-3}$. The Low Sage station that has

368 average stone contents of 0.16 $m^3 m^{-3}$, exhibited a slight reduction in cumulative ET_A, about
369 4% and 10% when considering stony soil with negligibly porous and highly porous stones.
370 Similarly, the Beaver Divide station with average stone content of 0.18 $m^3 m^{-3}$ showed
371 reduction in ET_A by nearly 3% while assuming highly porous stone and by 7% assuming
372 negligibly porous stones for both years. In contrast, the ET_A simulations for Beaver Divide
373 in 2016 showed incremental changes when considering either stone type.

374 **5. Discussion**

375 **5.1 Soil Moisture Dynamics and Model Calibration**

376 The inverse simulation was executed based on the goodness of fit between the measured
377 and simulated soil moisture, however the measured soil moisture may not directly include
378 and therefore represent stone content within the sensing volume. The ability of soil
379 moisture sensors to account for the stone content is limited by their sensing volume (Vaz
380 et al., 2013) and by the size of the surrounding stones (Coppola et al., 2013). In our study,
381 soil moisture sensors were generally installed as to intentionally avoid stones around
382 sensors. Hence measurements directly report soil moisture content of the soil matrix
383 without stone content and therefore, calibration of the soil hydraulic parameters in the
384 HYDRUS-1D numerical model was performed without directly accounting for the stone
385 content. The HYDRUS-1D model was able to simulate the soil moisture remarkably well
386 in all five stations with significant correlation of R^2 greater than 0.8 and RMSE less than
387 0.04 $m^3 m^{-3}$. These estimates were averaged over depths at all five stations for both years
388 (Table 3). Some discrepancies were observed such as at the 20 cm depth in Beaver Divide
389 and Soapstone, which showed relatively low R^2 of 0.651 and high RMSE of 0.05 $m^3 m^{-3}$
390 and 0.04 $m^3 m^{-3}$, respectively. The source of discrepancies between measured and

391 simulated soil moisture is likely due to the limited information available to the HYDRUS-
392 1D model to account for the complexity caused by soil heterogeneity, stone content or
393 preferential flow, which is quite common in forest soil (Flinn and Marks, 2007; Hawley et
394 al., 1983). Although the soil texture and stone content varied considerably within the
395 examined soil profiles, the simulation domains (2m deep) were clustered into five distinct
396 layers based on textural information obtained from the soil pit description. This
397 simplification of soil representation is a likely source of increased simulation error for soil
398 moisture.

399 **5.2 Simulation of Actual Evapotranspiration**

400 The HYDRUS-1D simulation for 2015 and 2016 suggested that the ET_A was strongly
401 correlated to the soil moisture availability during the growing season as 2016 showed lower
402 cumulative ET_A corresponding to the drier soil profile (Figure 4; 5; 8). The ET_A measured
403 by the eddy covariance system at the Low Sage station and simulated by HYDRUS-1D
404 followed the same trend (Figure 6). However, the model overestimated the peak values
405 noticeably, usually after the rain events in 2015. Despite the difference between spatial
406 scales of the eddy covariance footprint and the point scale simulation of HYDRUS-1D, the
407 results validate the potential of quantifying ET_A using soil moisture dynamics in natural
408 settings.

409 Slight differences between modeled daily ET_A and values measured by eddy covariance
410 were expected. The eddy covariance method does not always provide energy balance
411 closure consistently, which may lead to underestimation of latent heat flux or ET_A (Wilson
412 et al., 2002). When comparing the sum of latent heat flux and sensible heat with available
413 energy (Rn - G), Wilson et al. (2002) reported an average error of 20% from 22 FLUXNET

(an eddy covariance network) sites. Although the energy budget ratio at the Low Sage site over the two years during snow-free, non-freezing periods was 0.96, weekly values over the simulation period in Figure 6 were as low as 0.80. Moreover, error in HYDRUS-1D simulation may result from inaccuracy of model parameterization of soil hydraulics. Soils in natural settings are highly heterogeneous within the profile with extremely variable hydraulic properties. Limitations in the information representing soil and vegetation complexity might have resulted in incorrect estimations of water balance leading to erroneous ET_A estimates in some cases.

5.3 Accounting for Stone Content

The magnitude of the effects of stone content on the ET_A simulation was dependent upon the types of stone and their hydraulic properties. As presented in Durner (1994), prediction of both the water retention and hydraulic conductivity function near saturation may be highly unreliable and subject to large estimation error with even the best quality measurements. Acknowledging this, we assumed the saturated hydraulic conductivity of the stony soil was similar to that of the fine soil matrix while the unsaturated hydraulic conductivity for stony soil was defined by Eq. (14) as a function of effective saturation. Several studies suggest reduction in hydraulic conductivity due to increase in stone content, while conversely, the hydraulic conductivity has also been shown to increase in stony soil near saturation (Beckers et al., 2016; Sauer and Logsdon, 2002). Our simulation for low porosity stone tended to simulate ET_A that matched well with the eddy covariance estimates (Figure 6). Simulation of stony soil with negligibly porous stone reduced the total cumulative ET_A considerably at all five stations for both years except for Knowlton Fork,

437 which exhibited the lowest average stone content (Figure 2). However, the high porosity
438 stone, with water retention behavior similar to coarse sandstone, had the least effect on
439 ET_A simulation in comparison to the ET_A estimated without accounting for the stone
440 content. The cumulative ET_A over the simulation period was reduced by up to 30% for the
441 Soapstone site in 2016 when assuming negligibly porous stones (Table 5). This correlates
442 well with results in Cousin et al. (2003) that showed overestimation of available water
443 content by 39% when the presence of stones were not accounted for in soil.

444 **6. Conclusion**

445 In this study we demonstrated the influence of soil stone content on the uptake of water as
446 evapotranspiration (ET) from a mixture of grass and sagebrush using stony-soil moisture
447 dynamics. The soil moisture and ET_A simulated by HYDRUS-1D were found to be in good
448 agreement with directly measured soil moisture and ET_A using the eddy covariance system
449 indicating that the model is efficient in simulating the boundary fluxes including ET_A. The
450 simulated root water uptake from stony soil was found to be sensitive to stone content.
451 Simulation results revealed a significant reduction in cumulative ET_A of up to 30% percent
452 of total ET_A computed without accounting for the stone content. The simulated ET_A values
453 were least affected when considering soil with highly porous stones, while estimates were
454 reduced significantly for the stations with higher average stone content, when considering
455 soil with negligibly porous stones. Numerical simulations revealed that lower- and higher-
456 porosity stones reduced ET_A by 30% and 10%, respectively, highlighting the potential for
457 overestimation of ET_A when stone content is neglected in modeling. It is hence important
458 to incorporate hydraulic properties of stones to more accurately estimate ET_A by
459 accounting for stone impact on soil moisture dynamics in stony soil. This study provides

guidelines and tools for numerical simulation of soil moisture dynamics for improved estimation of ET_A from stony soils such as are commonly found in montane forest ecosystems.

7. Acknowledgements

We express appreciation to Christopher Cox, Jobie Carlisle and John Lawley who provided technical support. This research was supported by the iUTAH project funded through an NSF EPSCoR grant EPS 1208732 awarded to Utah State University, as part of the State of Utah Research Infrastructure Improvement Award. Additional support was provided by the Utah Agricultural Experiment Station, Utah State University, Logan, Utah 84322-4810, approved as UAES journal paper no. 9101. Any opinions, findings, and conclusions or recommendations expressed are those of the author(s) and do not necessarily reflect the views of the National Science Foundation.

References

Allen, R. G., Pereira, L. S., Raes, D., and Smith, M. (1998). Crop evapotranspiration-Guidelines for computing crop water requirements-FAO Irrigation and drainage paper 56. *FAO, Rome*, *300*(9), D05109.

Andréassian, V. (2004). Waters and forests: from historical controversy to scientific debate. *J. Hydrol.*, *291*(1-2), 1-27.

Baldocchi, D. D., and Ryu, Y. (2011). A Synthesis of Forest Evaporation Fluxes –from Days to Years – as Measured with Eddy Covarience. In *Forest Hydrology and Biogeochemistry: Synthesis of Past Research and Future Directions* (Vol. 216, pp. 101-116). Springer.

Baldocchi, D. D., Hincks, B. B., and Meyers, T. P. (1988). Measuring Biosphere-Atmosphere Exchanges of Biologically Related Gases with micrometeeorological methods. *Ecology*, 69(5), 1331-1340.

485 Beckers, E., Pichault, M., Pansak, W., Degré, A., and Garré, S. (2016). Characterization of
486 stony soils' hydraulic conductivity using laboratory and numerical
487 experiments. *Soil*, *2*(3), 421-431.

488 Blonquist, J.M.J., Jones, S.B., Robinson, D.A., (2005). Standardizing characterization of
489 electromagnetic water content sensors. *Vadose Zone J*. 4(4): 1059-1069.

490 Cai, X., Pan, M., Chaney, N. W., Colliander, A., Misra, S. and Cosh, M. H. et al. (2017).
491 Validation of SMAP soil moisture for the SMAPVEX15 field campaign using a
492 hyper-resolution model. *Water Resour. Res.*, *53*(4), 3013-3028.

493 Coppola, A., Dragonetti, G., Comegna, A., Lamaddalena, N., Caushi, B., Haikal, M.A.,
494 Basile, A. (2013). Measuring and modeling water content in stony soils. *Soil Tillage*
495 *Res.,* 128, 9-22.

496 Cousin, I., Nicoullaud, B., and Coutadeur, C. (2003). Influence of rock fragments on the
497 water retention and water percolation in a calcerous soil. *Catena* (53), 97-114.

498 Durner, W. (1994). Hydraulic conductivity estimation for soils with heterogeneous pore
499 structure. *Water Resour. Res.*, *30*(2), 211-223.

500 Feddes, R. A., Bresler, E., and Neuman, S. P. (1974). Field test of a modified numerical
501 model for water uptake by root systems. *Water Resour. Res.*, *10*(6), 1199-1206.

502 Feddes, R. A., Kowalik, P. J., and Zaradny, H. (1978). *Simulation of field water use and*
503 *crop yield*. Centre for Agricultural Publishing and Documentation.

504 Feddes, R. A., Hoff, H., Bruen, M., Dawson, T., de Rosnay, P., Dirmeyer, P., and Pitman,
505 A. J. (2001). Modeling root water uptake in hydrological and climate models. *Bull.*
506 *Am. Meteorol. Soc.*, *82*(12), 2797-2809.

507 Fellows, A. W. Flerchinger, G N., Seyfried, M. S., and Lohse, K. (2017). *Data for*
508 *Partitioned Carbon and Energy Fluxes Within the Reynolds Creek Critical Zone*
509 *Observatory* [Data set]. Retrieved from https://doi.org/10.18122/B2TD7V

510 Finzel, J. A., Seyfried, M. S., Weltz, M. A., Kiniry, J. R., Johnson, M. V. V., and
511 Launchbaugh, K. L. (2012). Indirect measurement of leaf area index in Sagebrush-
512 Steppe Rangelands. *Rangeland Ecol. Manag.*, *65*(2), 208-212.

513 Food and Agriculture Organization (FAO) of the United Nations (1990). Expert
514 consultation on revision of FAO methodologies for crop water requirements,
515 ANNEX V, FAO Penman-Monteith Formula, Rome, Italy.

516 Flinn, K.M., Marks, P.L., 2007. Agricultural legacies in forest environments: tree
517 communities, soil properties, and light availability. *Ecol. Appl.* 17(2): 452-463.

518 Hargreaves, G. H., and Samani, Z. A. (1985). Reference crop evapotranspiration from
519 temperature. *Appl. Eng. Agric*, *1*(2), 96-99.

520 Hawley, M.E., Jackson, T.J., McCuen, R.H., 1983. Surface soil moisture variation on small
521 agricultural watersheds. *J. Hydrol.* 62(1–4): 179-200.

522 Hilten, R. N., Lawrence, T. M., and Tollner, E. W. (2008). Modeling stormwater runoff
523 from green roofs with HYDRUS-1D. *J. Hydrol.* , *358*(3-4), 288-293.

524 Hlavacikova, H., and Novak, V. (2013). Comparison of daily potential evapotranspiration
525 calculated by two procedures based on Penman-Monteith type equation. *J. Hydrol.*
526 *Hydromechanics*, *61*(2), 173-176.

527 Hlavacikova, H., Novak, V., and Simunek, J. (2016). The effects of rock fragment shapes
528 and positions on modeled hydraulic conductivities of stony soils. *Geoderma*, *281*,
529 39-48.

530 Hoffman, G. J., and van Genuchten, M. T. (1983). Soil properties and efficient water use:
531 water management for salinity control. *Limitations to efficient water use in crop*
532 *production*, (*limitations to ef.*), 73-85.

533 Ice, G. G., and Stednick, J. D. (2004). A century of forest and wildland watershed lessons.
534 Bethesda, MD: *Society of American Foresters*.

535 iUTAH GAMUT Working Group . (2014). iUTAH GAMUT Network Raw Data.
536 Retrieved from iUTAH Modeling and Data Federation:
537 http://repository.iutahepscor.org/dataset/

538 Izadifar, Z., and Elshorbagy, A. (2010). Prediction of hourly actual evapotranspiration
539 using neural networks, genetic programming, and statistical models. *Hydrol.*
540 *Processes*, *24*(23), 3413-3425.

541 Jones, A.S., Z.T. Aanderud, J.S. Horsburgh, D. Eiriksson, D. Dastrup, and C. Cox et al.
542 (2017). Designing and Implementing a Network for Sensing Water Quality and
543 Hydrology across Mountain to Urban Transitions. *J. Am. Water Resour. Assoc.*
544 53(5):1095–1120. https://doi.org/10.1111/1752-1688.12557

545 Jones, S.B., Blonquist, J.M., Robinson, D.A., Rasmussen, V.P., Or, D., (2005).
546 Standardizing characterization of electromagnetic water content sensors. *Vadose*
547 *Zone J.,* 4(4): 1048-1058.

548 Kool, D., Agam, N., Lazarovitch, N., Heitman, J. L., Sauer, T. J., and Ben-Gal, A. (2014).
549 A review of approaches for evapotranspiration partitioning. *Agric. For.*
550 *Meteorol., 184*, 56-70.

551 Koster, R. D., Dirmeyer, P. A., Guo, Z., Bonan, G., Chan, E., and Cox, P. et al. (2004).
552 Regions of strong coupling between soil moisture and
553 precipitation. *Science*, *305*(5687), 1138-1140.

554 Kumar, S. V., Peters-Lidard, C. D., Tian, Y., Houser, P. R., Geiger, J., Olden, S., ... and
555 Adams, J. (2006). Land information system: An interoperable framework for high
556 resolution land surface modeling. *Environ. Model Softw.*, *21*(10), 1402-1415.

557 Law, B. E., Falge, E., Gu, L. V., Baldocchi, D. D., Bakwin, P., Berbigier, P., ... and
558 Goldstein, A. (2002). Environmental controls over carbon dioxide and water vapor
559 exchange of terrestrial vegetation. *Agric. For. Meteorol.*, *113*(1), 97-120.

560 Lv, L., Franz, T. E., Robinson, D. A., and Jones, S. B. (2014). Measured and Modeled Soil
561 Moisture Compared with Cosmic-Ray Neutron Probe Estimates in a Mixed
562 Forest. *Vadose Zone J.*, *13*(12), vzj2014-06.

563 Miyazawa, Y., Kobayashi, N., Mudd, R. G., Tateishi, M., Lim, T., and Mizoue, N. et al.
564 (2013). Leaf and soil-plant hydraulic processes in the transpiration of tropical
565 forest. *Procedia Environmental Sciences*, *19*, 77-85.

566 Mohanty, B. P. (2013). Soil hydraulic property estimation using remote sensing: A
567 review. *Vadose Zone J.*, *12*(4).

568 Monteith, J., and Unsworth, M. (2007). *Principles of environmental physics*. Academic
569 Press.

570 Mu, Q., Heinsch, F. A., Zhao, M., and Running, S. W. (2007). Development of a global
571 evapotranspiration algorithm based on MODIS and global meteorology data.
572 *Remote Sens. Environ.*, 111(4), 519-536.

573 Mualem, Y. (1976). A new model for predicting the hydraulic conductivity of unsaturated
574 porous media. *Water Resour. Res.,* 12, 513–522.

575 Niu, G. Y., Yang, Z. L., Mitchell, K. E., Chen, F., Ek, M. B., and Barlage, M. et al. (2011).
576 The community Noah land surface model with multiparameterization options
577 (Noah-MP): 1. Model description and evaluation with local-scale measurements. *J.*
578 *Geophys. Res. Atmos.*, *116*(D12).

579 Novak, V., and Knava, K. (2012). The influence of stoniness and canopy properties on soil
580 water content distribution: simulation of water movement in forest stony soil. *Eur.*
581 *J. Forest Res.*, 131(6), 1727–1735.

582 Novak, V., Knava, K., and Simunek, J. (2011). Determining the influence of stones on
583 hydraulic conductivity of saturated soils using numerical method. *Geoderma* (161),
584 177-181.

585 Parajuli, K. (2015). Spatial Analysis of Actual Evapotranspiration Estimates from the
586 iUTAH Climate Station Network. In *World Environmental and Water Resources*
587 *Congress 2015* (pp. 2252-2260). https://doi.org/10.1061/9780784479162.222

588 Parajuli, K., Sadeghi, M., and Jones S. B. (2017a). A binary mixing model for
589 characterizing stony-soil water retention. *Agric. For. Meteorol.*, *244*, 1-8.

590 Parajuli, K., S. B. Jones and J. Lawley (2017b). Soil Description for GAMUT Weather
591 Stations, *HydroShare*,
592 http://www.hydroshare.org/resource/4dc603691c964c07a766f00638024776

593 Parajuli, K. (2018). Advancing Methods to Quantify Actual Evapotranspiration in Stony
594 Soil Ecosystems. *All Graduate Theses and Dissertations*. 7242.
595 https://digitalcommons.usu.edu/etd/7242

596 Parajuli, K., L. Zhao, S. B. Jones, D. G. Tarboton, M. Sadeghi, L. E. Hipps, A. Torres-Rua,
597 and G. N. Flerchinger (2019). Noah-MP simulations of evapotranspiration and
598 moisture dynamics in stony soil (Submitted to *Agric. For. Meteorol.*)

599 Patton, N. R.; Lohse, K. A.; Seyfried, M. S.; Will, R. M.; and Benner, S. (2018). *Dataset*
600 *for Coarse Fraction Adjusted Bulk Density Estimates for Dryland Soils Derived*
601 *from Felsic and Mafic Parent Materials* [Data set]. Retrieved from
602 https://doi.org/10.18122/B22M6Q

603 Prueger, J. H., Hatfield, J. L., Aase, J. K., and Pikul, J. L. (1997). Bowen-ratio comparisons
604 with lysimeter evapotranspiration. *Agron. J.*, *89*(5), 730-736.

605 Raziei, T., and Pereira, L. S. (2013). Estimation of ETo with Hargreaves–Samani and FAO-
606 PM temperature methods for a wide range of climates in Iran. *Agric. Water*
607 *Manage., 121*, 1-18.

608 Richards, L. A. (1931). Capillary conduction of liquids through porous mediums. *J. Appl.*
609 *Phys.*, 1(5), 318-333.

610 Ries, F., Lange, J., Schmidt, S., Puhlmann, H., and Sauter, M. (2015). Recharge estimation
611 and soil moisture dynamics in a Mediterranean, semi-arid karst region. *Hydrol.*
612 *Earth Syst. Sci.*, *19*(3), 1439-1456.

613 Ritchie, J. T. (1972). Model for predicting evaporation from a row crop with incomplete
614 cover. *Water Resour. Res.*, *8*(5), 1204-1213.

615 Sadeghi M., Tuller M., Warrick A. W., Babaeian E., Parajuli K., Gohardoust M. R., Jones
616 S. B., (2019). An analytical model for estimation of land surface net water flux from
617 near-surface soil moisture observations. *J. Hydrol.*

618 Sauer, T. J., and Logsdon, S. D. (2002). Hydraulic and physical properties of stony soils in
619 a small watershed. *Soil Sci. Soc. Am. J.*, *66*(6), 1947-1956.

620 Schelde, K., Ringgaard, R., Herbst, M., Thomsen, A., Friborg, T., and Søgaard, H. (2011).
621 Comparing evapotranspiration rates estimated from atmospheric flux and TDR soil
622 moisture measurements. *Vadose Zone J.,* 10:78-83

623 Senay, G. B., Leake, S., Nagler, P. L., Artan, G., Dickinson, J., and Glenn, J. T. (2011).
624 Estimating basin scale evapotranspiration (ET) by water balance and remote
625 sensing methods. *Hydrol. Processes, 25*, 4037-4049.

626 Sheffield, J., Wood, E. F., and Arriola, F. M. (2010). Long-Term Regional Estimates of
627 Evapotranspiration for Mexico Based on Downscaled ISCCP Data. *J.*
628 *Hydrometeorol., 11*, 253-275.

629 Simunek, J., M. Sejna, H. Saito, M. Sakai, and M. Th. van Genuchten. (2013). The
630 HYDRUS-1D Software Package for Simulating the Movement of Water, Heat, and
631 Multiple Solutes in Variably Saturated Media, Version 4.17, *HYDRUS Software*
632 *Series 3*, Department of Environmental Sciences, University of California
633 Riverside, Riverside, California, USA, pp. 343.

634 Simunek, J., van Genuchten, M. T., and Sejna, M. (2016). Recent developments and
635 applications of the HYDRUS computer software packages. *Vadose Zone J.*, *15*(7).

636 Soylu, M. E., Istanbulluoglu, E., Lenters, J. D., and Wang, T. (2011). Quantifying the
637 impact of groundwater depth on evapotranspiration in a semi-arid grassland
638 region. *Hydrol. Earth Syst. Sci.*, *15*(3), 787-806.

639 Sun, G., Noormets, A., Chen, J., and McNulty, S. G. (2008). Evapotranspiration estimates
640 from eddy covariance towers and hydrologic modeling in managed forests in
641 Northern Wisconsin, USA. *Agric. For. Meteorol.*, *148*(2), 257-267.

642 Sutanto, S. J., Wenninger, J., Coenders-Gerrits, A. M. J., and Uhlenbrook, S. (2012).
643 Partitioning of evaporation into transpiration, soil evaporation and interception: a
644 comparison between isotope measurements and a HYDRUS-1D model. *Hydrol. Earth*
645 *Syst. Sci.*, *16*(8), 2605-2616.

646 Tetegan, M., Nicoullaud, B., Baize, D., Bouthier, A., and Cousin, I. (2011). The contribution
647 of rock fragments to the available water content of stony soils: Proposition of new
648 pedotransfer functions. *Geoderma* (165), 40-49.

649 Topp, G.C., Davis, J.L., Annan, A.P., 1980. Electromagnetic determination of soil water
650 content: Measurements in coaxial transmission lines. *Water Resour. Res.* 16(3): 574-
651 582.

652 Ugolini F.C., Corti G., Agnelli A., Certini G. (1998) Under- and overestimation of soil
653 properties in stony soils. *16th World Congress of Soil Science*, Montpellier

654 van Genuchten, M. T. (1980). A closed-form equation for predicting the hydraulic conductivity
655 of unsaturated soils. *Soil Sci. Soc. Am. J.*, *44*(5), 892-898.

656 Vaz, C.M., Jones, S., Meding, M. and Tuller, M., 2013. Evaluation of standard calibration
657 functions for eight electromagnetic soil moisture sensors. *Vadose Zone J.*, *12*(2).

658 Wilcox, B. P., Breshears, D. D., and Allen, C. D. (2003). Ecohydrology of a resource-
659 conserving semiarid woodland: Effects of scale and disturbance. *Ecol.*
660 *Monographs*, *73*(2), 223-239.

661 Wilson, K. B., Hanson, P. J., Mulholland, P. J., Baldocchi, D. D., and Wullschleger, S. D.
662 (2001). A comparison of methods for determining forest evapotranspiration and its

components: sap-flow, soil water budget, eddy covariance and catchment water balance. *Agric. For. Meteorol.*, *106*(2), 153-168.

Wilson, K., Goldstein, A., Falge, E., Aubinet, M., Baldocchi, and D., Berbigier, et al. (2002). Energy balance closure at FLUXNET sites. *Agric. For. Meteorol., 113*(1), 223-243.

Yang, Z. L., Niu, G. Y., Mitchell, K. E., Chen, F., Ek, M. B., and Barlage, M et al. (2011). The community Noah land surface model with multiparameterization options (Noah-MP): 2. Evaluation over global river basins. *J. Geophys. Res. Atmos.*, *116* (D12).

Zhou, Guoyi, Ge Sun, Xu Wang, Chuanyan Zhou, Steven G. McNulty, James M. Vose, and Devendra M. Amatya, (2008). Estimating Forest Ecosystem Evapotranspiration at Multiple Temporal Scales With a Dimension Analysis Approach. *J Am. Water Works Assoc.*, 44(1):208-221. DOI: 10.1111/j.1752-1688.2007.00148.x

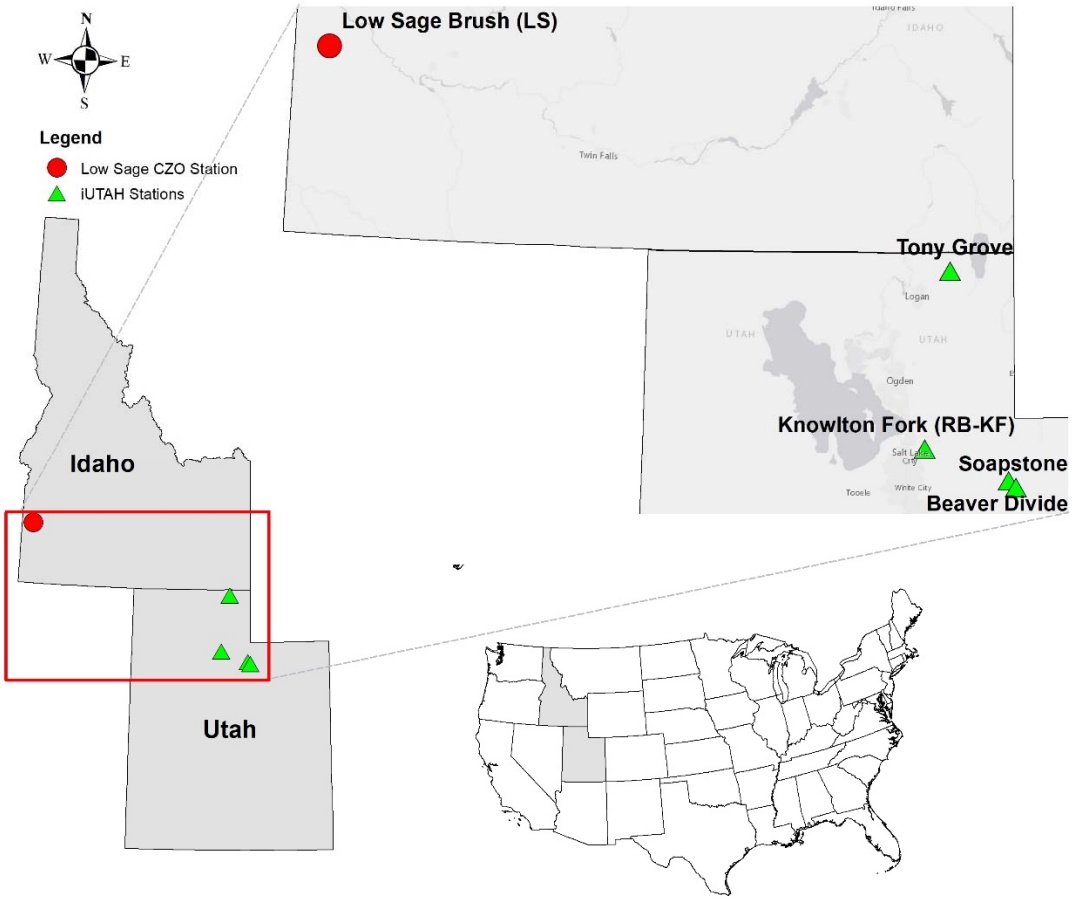

678

679 Figure 1. Selected climate stations in Northern Utah and Reynolds Creek, Idaho installed
680 by iUTAH and the Critical Zone Observatory (CZO) respectively. All stations have
681 measurements of meteorological parameters including volumetric soil water content. The
682 Low Sage station is furthermore equipped with an eddy covariance tower.

683

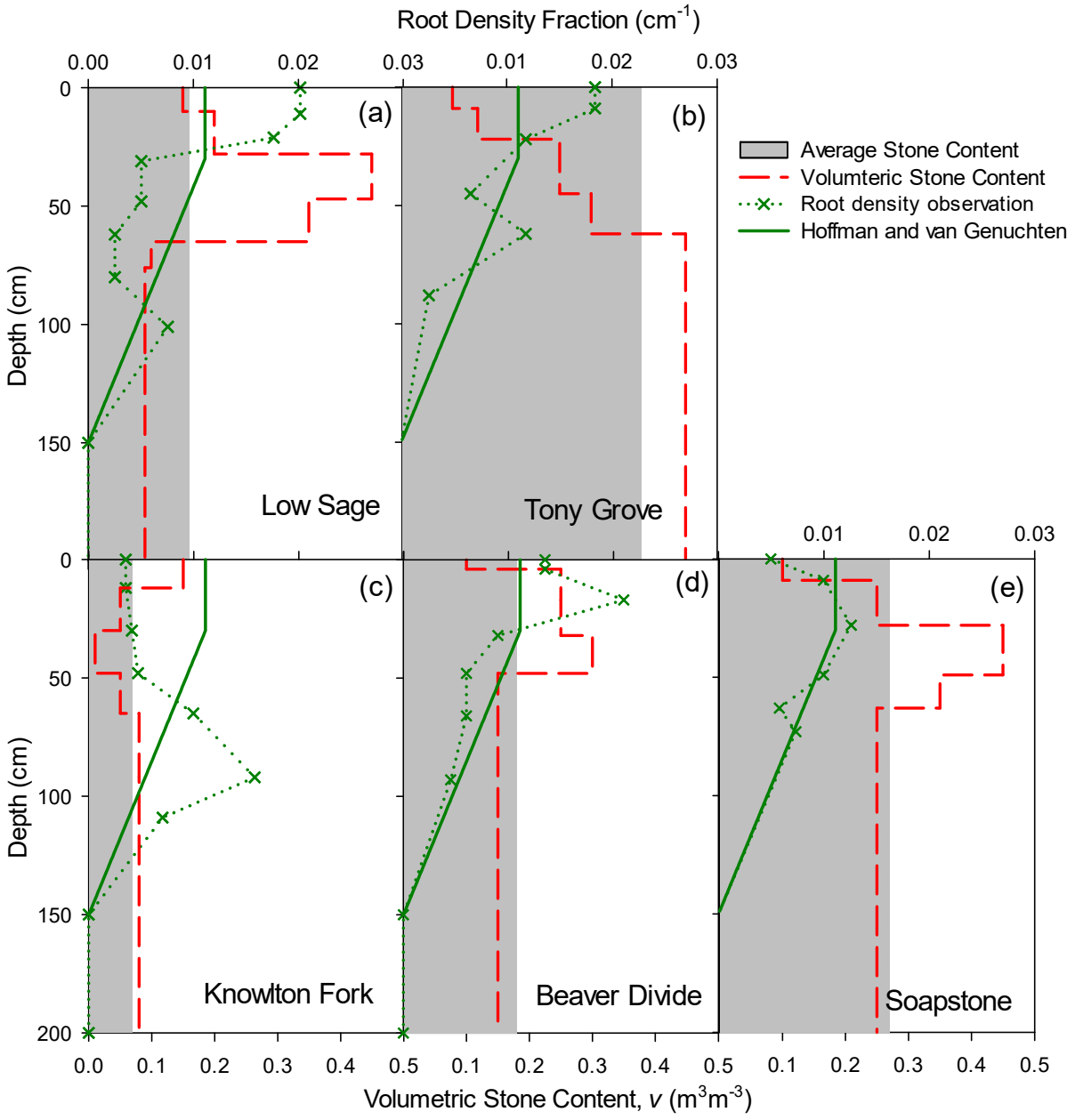

684

685 Figure 2. Root density distribution and volumetric stone content along the soil profile at
686 (a) Low Sage, (b) Tony Grove, (c) Knowlton Fork, (d) Beaver Divide and (e) Soapstone
687 weather stations. The root density distribution was estimated based on root counts from
688 soil pit description and compared with Hoffman and van Genuchten (1983) method. The
689 stone content were obtained from the soil pit description during the installation of climate
690 stations. Information on stone content was available to the depth of around 100 cm.
691 Below that depth the stone content is considered similar to the stone content in the bottom
692 most layer from the soil pit description. The average stone content is taken from stone
693 distribution in the entire 200 cm soil profile.

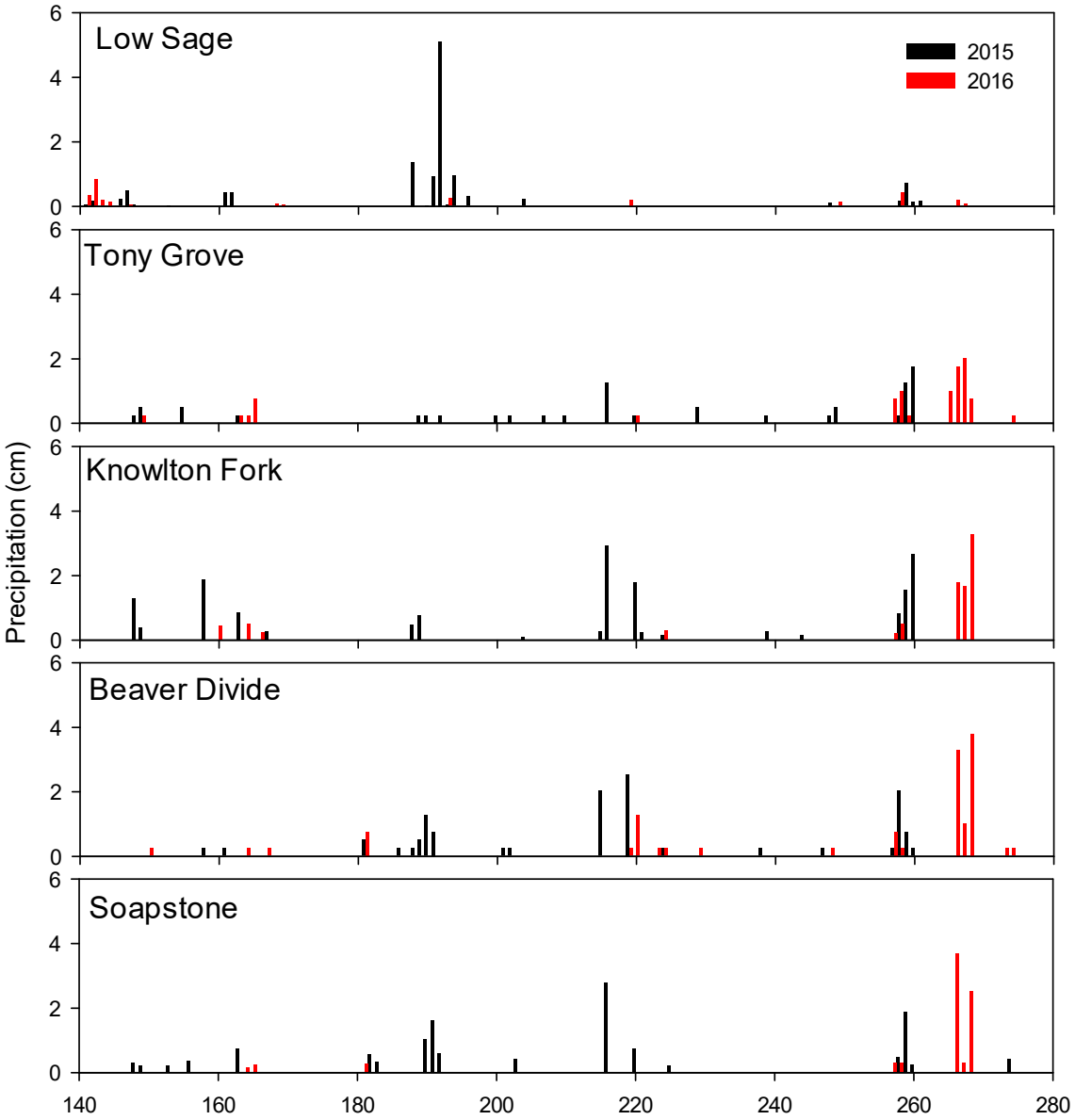

694

695 Figure 3. Daily precipitation during the HYDRUS-1D simulation period in the selected
696 sites for 2015 and 2016.

697

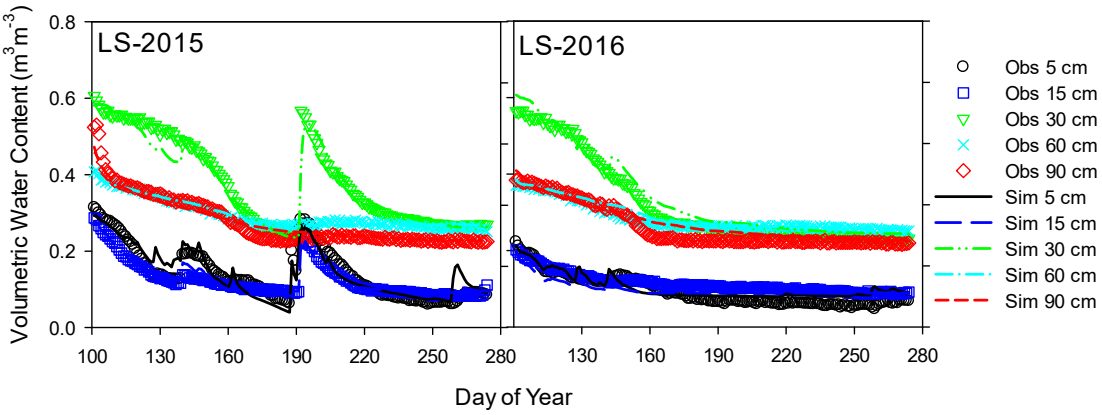

698

699 Figure 4. Volumetric water content reported by Hydraprobe sensors (points) at different
700 depths and as simulated by HYDRUS-1D (lines) after calibration for the growing seasons
701 of 2015 and 2016 at the low sage station. The simulation period was between DOY 100
702 (10 April) and DOY 273 (30 September).

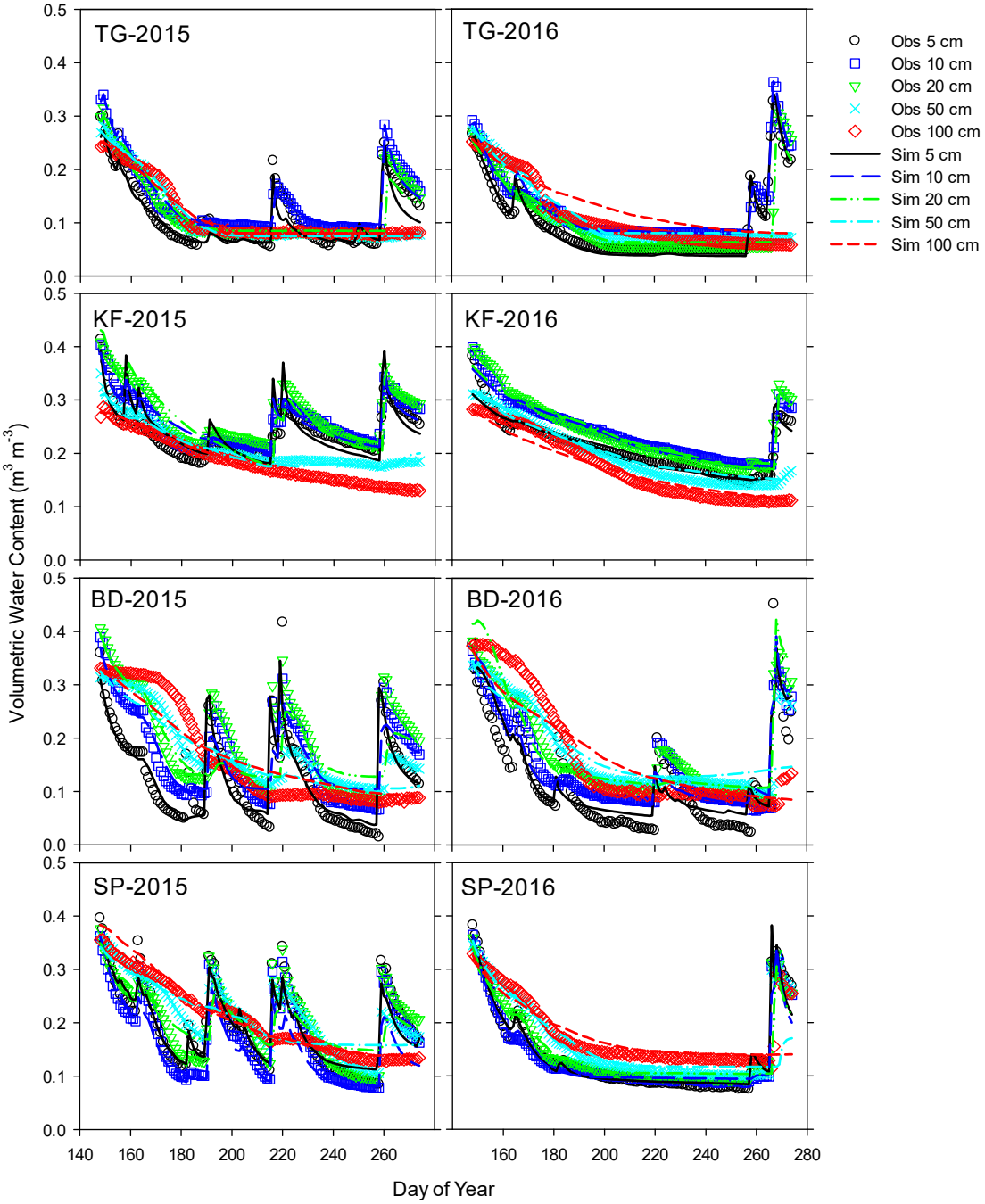

Figure 5. Volumetric water content reported by TDT sensor (points) at different depths and as simulated by HYDRUS-1D (lines) after calibration for the growing season of 2015 and 2016 at Tony Grove (TG), Knowlton Fork (KF), Beaver Divide (BD) and Soapstone (SP). The simulation period was between DOY 147 (27 May) and DOY 273 (30 September).

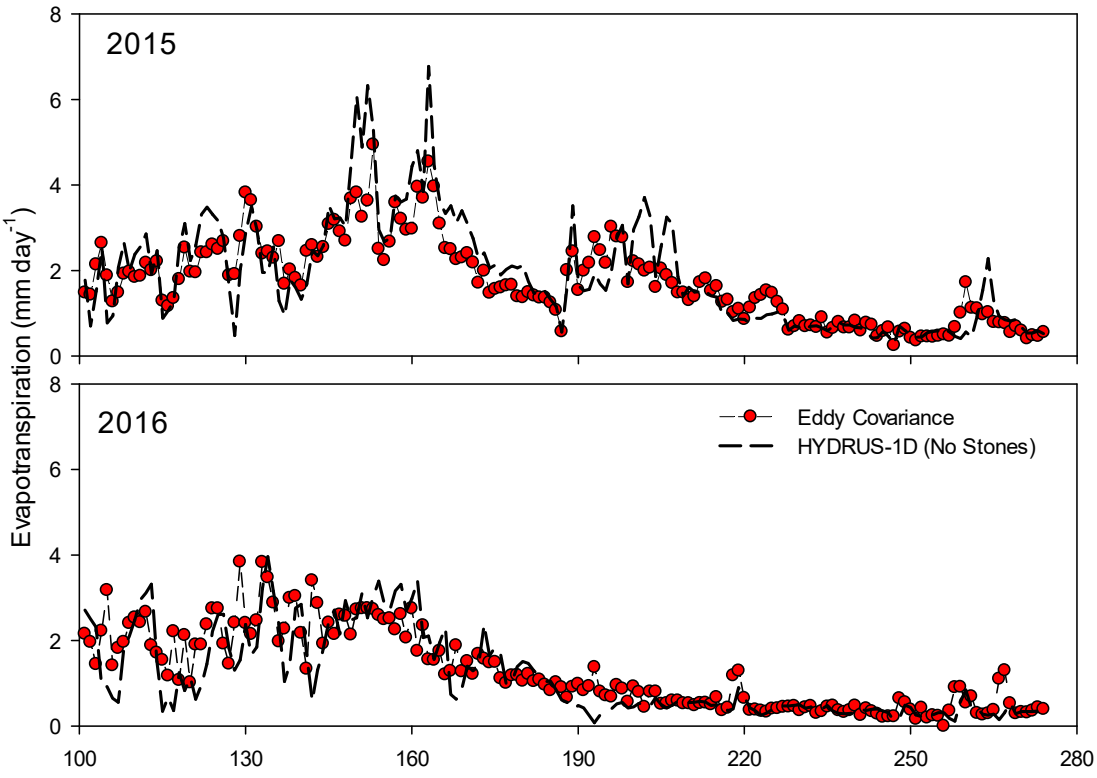

Figure 6. Actual evapotranspiration measurements from the eddy covariance system compared with actual evapotranspiration simulated using HYDRUS-1D without accounting for stone content at the Low Sage station in Reynolds Creek Experimental Watershed for the year 2015 and 2016.

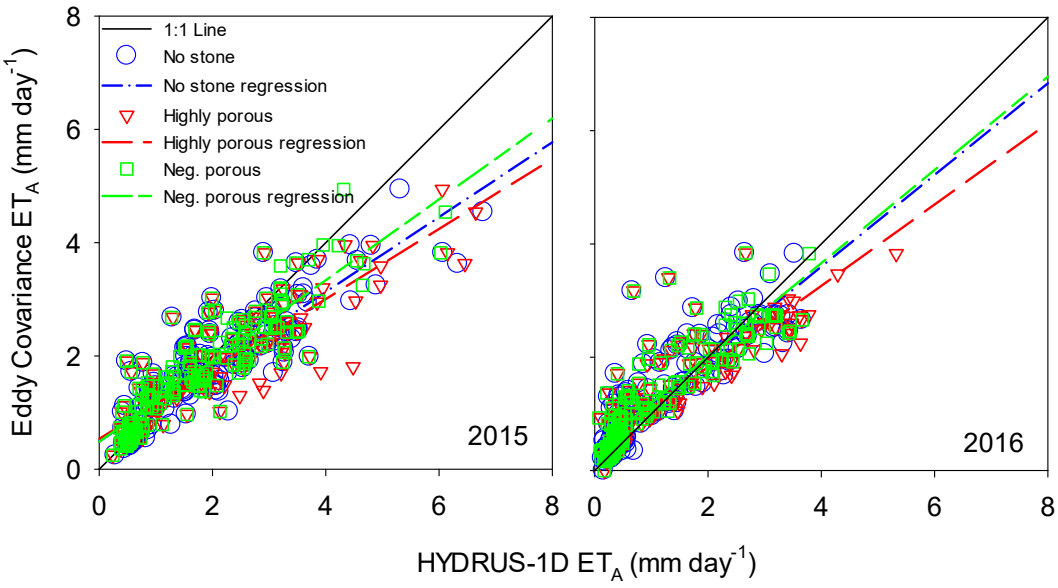

716

717 Figure 7. Scatter plot between the evapotranspiration measured by the Eddy Covariance
718 tower at the low sage station and the HYDRUS-1D simulations of actual
719 evapotranspiration assuming no stones, highly porous and negligibly porous stones along
720 with their regression line for 2015 and 2016.

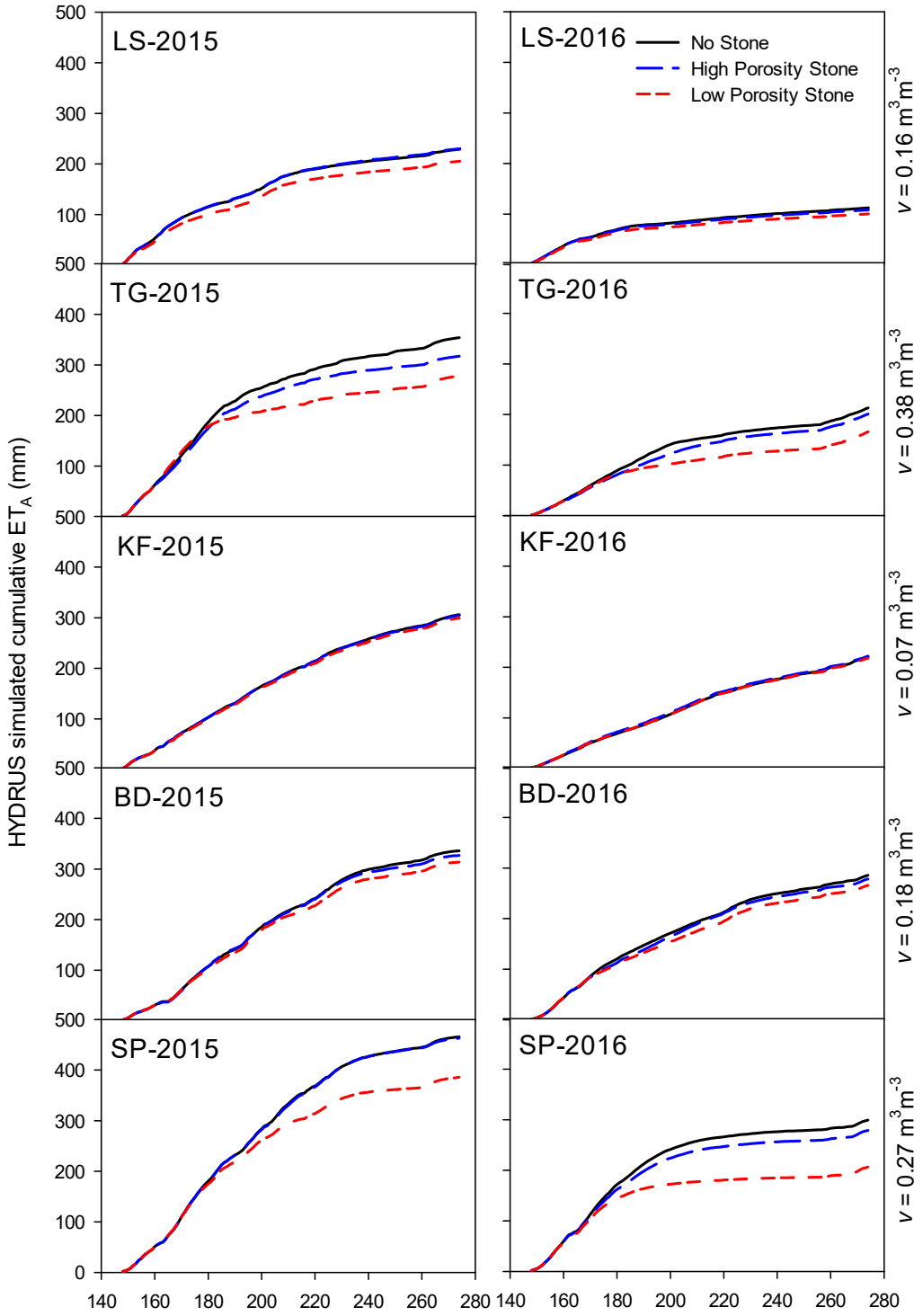

Figure 8. Cumulative evapotranspiration simulated by HYDRUS-1D under three different scenarios considering soil with -no stone, -highly porous stone and -negligibly porous stone at the Low Sage (LS), Tony Grove (TG), Knowlton Fork (KF), Beaver Divide (BD) and Soapstone (SP) stations for 2015 and 2016. The ET is cumulative from DOY 148 (28 May) to DOY 273 (30 September). The stone content along the soil profile is presented in Figure 2. Average stone content (v) for each site is presented on the right side of each plot.

729 Table 1. Location and description of weather stations with major vegetation types and
730 maximum LAI used in this study. The maximum LAI value for Low Sage weather station
731 was taken from Finzel et al. (2012) while at the iUTAH stations LAI was determined
732 from measurements of a Line Quantum Meter (MQ-301, Apogee).
733

Station	Latitude	Longitude	Elevation (m)	Vegetation	LAI_{Max}
Low Sage (LS)	43.14	-116.74	1608	Sagebrush	2.30
Tony Grove (TG)	41.89	-111.57	1928	Sagebrush, Grass	2.20
Knowlton Fork (KF)	40.81	-111.77	2178	Grass, Fern	4.50
Beaver Divide (BD)	40.61	-111.10	2508	Sagebrush, Grass	1.20
Soapstone (SP)	40.57	-111.04	2388	Sagebrush, Grass	2.30

734

735

736 Table 2. Measured water retention parameters: saturated water content (θ_s), residual water
737 content (θ_r), shape parameters α and n for the stone fragments obtained from Parajuli et
738 al., (2017).
739

Parameters	Highly Porous Stone (Coarse Sandstone)	Negligibly Porous Stones (Fine Sandstone)
θ_s [$m^3\ m^{-3}$]	0.28	0.036
θ_r [$m^3\ m^{-3}$]	0.012	0
α [m^{-1}]	0.032	0.084
n	2.115	1.219

740

Table 3. Goodness of fit for measured soil moisture content with the HYDRUS-1D simulation, expressed in terms of the coefficients of determination (R^2) and root mean squared errors (RMSE)

Year	Sensor Depth	Low Sage		Sensor Depth	Tony Grove		Knowlton Fork		Beaver Divide		Soapstone	
		R^2	RMSE ($m^3\ m^{-3}$)		R^2	RMSE ($m^3\ m^{-3}$)	R^2	RMSE ($m^3\ m^{-3}$)	R^2	RMSE ($m^3\ m^{-3}$)	R^2	RMSE ($m^3\ m^{-3}$)
2015	5 cm	0.853	0.025	5 cm	0.927	0.021	**0.667**	0.028	**0.671**	**0.047**	0.927	0.025
	15 cm	0.931	0.013	10 cm	0.951	0.014	0.853	0.017	0.889	**0.032**	0.873	**0.035**
	30 cm	0.957	0.028	20 cm	0.903	0.019	0.839	0.025	**0.651**	**0.052**	**0.651**	**0.042**
	60 cm	0.975	0.006	50 cm	0.989	0.006	0.962	0.008	0.866	0.026	0.638	**0.039**
	90 cm	0.967	0.019	100 cm	0.976	0.009	0.994	0.005	0.936	**0.033**	0.976	0.014
	Average	0.937	0.018		0.949	0.014	0.863	0.017	0.803	**0.038**	0.813	0.031
2016	5 cm	0.817	0.016	5 cm	0.989	0.011	0.893	0.017	**0.771**	**0.044**	0.966	0.015
	15 cm	0.837	0.022	10 cm	0.990	0.007	0.974	0.010	0.875	0.030	0.978	0.012
	30 cm	0.984	0.026	20 cm	0.989	0.014	0.942	0.016	0.919	0.029	0.913	0.022
	60 cm	0.957	0.012	50 cm	0.985	0.012	0.986	0.012	0.807	**0.036**	**0.705**	**0.041**
	90 cm	0.935	0.022	100 cm	0.947	0.027	0.980	0.015	0.904	**0.040**	**0.707**	**0.034**
	Average	0.906	0.020		0.980	0.014	0.955	0.014	0.855	**0.036**	0.854	0.024

749 Table 4. Goodness of fit for evapotranspiration measured by eddy covariance with HYDRUS-
750 1D simulation considering soil with: (1) no stones, (2) highly porous stones, and (3) negligibly
751 porous stones, expressed in terms of coefficients of determination (R^2) and root mean squared
752 errors (RMSE)
753

	2015		2016	
	R^2	RMSE (mm/day)	R^2	RMSE (mm/day)
No Stone	0.78	0.64	0.76	0.51
Highly Porous Stone	0.76	0.73	0.78	0.54
Negligibly Porous Stone	0.79	0.55	0.79	0.49

754

Table 5. HYDRUS-1D simulated actual-Transpiration (T_A) , -Evaporation (E_A) and -Evapotranspiration (ET_A) reported as mm of water loss at different sites in years 2015 and 2016 under three different scenarios considering soil with no stones, highly porous stones and negligibly porous stones. The numbers on right hand side are percent change while considering the highly- and negligibly-porous stones as compared to no stone condition.

Year	Scenario	Component	Low Sage		Tony Grove		Knowlton Fork		Beaver Divide		Soapstone	
			(mm)	Change (%)	(mm)	Change (%)	(mm)	Change (%)	(mm)	Change (%)	(mm)	Change (%)
2015	No Stone	T_A	134		262		228		267		384	
		E_A	95		92		78		69		81	
		ET_A	229		354		306		336		466	
	Highly Porous Stone	T_A	130	*-3.06*	258	*-1.61*	226	*-0.84*	265	*-0.54*	384	*-0.22*
		E_A	101	*5.97*	59	*-35.27*	79	*0.84*	62	*-11.14*	80	*-2.36*
		ET_A	231	*0.70*	317	*-10.35*	305	*-0.41*	327	*-2.72*	463	*-0.60*
	Negligibly Porous Stone	T_A	124	*-6.97*	180	*-31.46*	228	*-0.12*	247	*-7.40*	307	*-20.22*
		E_A	81	*-14.57*	99	*7.25*	72	*-8.02*	67	*-3.62*	79	*-2.85*
		ET_A	206	*-10.13*	278	*-21.41*	299	*-2.14*	314	*-6.62*	386	*-17.19*
2016	No Stone	T_A	103		156		165		172		245	
		E_A	9		57		56		114		54	
		ET_A	112		213		221		286		299	
	Highly Porous Stone	T_A	99	*-4.56*	148	*-5.07*	163	*-1.44*	196	*14.02*	226	*-7.64*
		E_A	10	*10.17*	54	*-6.41*	60	*7.48*	83	*-27.56*	52	*-3.30*
		ET_A	109	*-3.38*	202	*-5.43*	222	*0.81*	278	*-2.58*	279	*-6.85*
	Negligibly Porous Stone	T_A	92	*-11.31*	111	*-28.76*	165	*-0.16*	180	*5.07*	160	*-34.74*
		E_A	9	*-0.52*	55	*-3.80*	54	*-3.45*	86	*-25.00*	47	*-13.80*
		ET_A	101	*-10.44*	166	*-22.05*	218	*-0.99*	266	*-6.94*	207	*-30.95*